Engineering Structures 195 (2019) 243–262

Contents lists available at ScienceDirect

Engineering Structures

journal homepage: www.elsevier.com/locate/engstruct

Effect of pounding on nonlinear seismic response of torsionally coupled steel structures resting on flexible soil

D. Farahani[a], F. Behnamfar[a,*], H. Sayyadpour[b]

[a] Department of Civil Engineering, Isfahan University of Technology, Esfahan 8415683111, Iran
[b] Faculty of Technology and Mining, Yasouj University, Choram 75761-59836, Iran

ARTICLE INFO

Keywords:
Soil-structure interaction
Pounding
Torsional eccentricity
Nonlinear response
Adjacent buildings

ABSTRACT

The effects of earthquake induced pounding on the nonlinear response of torsionally coupled buildings resting on flexible soil are investigated in the current study. Three steel moment-resisting frame buildings with the same symmetric plan having 4, 7 and 10 stories are considered. Three-dimensional nonlinear models with different eccentricity ratios are created. The soil-structure interaction phenomenon is taken into account using the Winkler beam on nonlinear springs. The pair of adjacent structures spaced at different clear distances resting on a flexible soil are analyzed under a consistent set of ground motion records and the effects of seismic pounding, torsional eccentricity and soil-structure interaction are studied by comparison of nonlinear dynamic responses of buildings. The results show that the peripheral frames experienced the most critical conditions during earthquake-induced pounding and the combined effect of soil-structure interaction, torsional eccentricity and pounding results in the most severe nonlinear responses of the studied buildings in certain cases.

1. Introduction

Adjacent buildings may experience seismic pounding during strong ground motions leading to impulse force being imposed on these structures. Such an extra force can alter the design forces and performance level of structures. As the seismic pounding phenomenon is substantially complicated, the building codes just set a seismic separation distance provision to completely avoid occurrence of pounding.

Many efforts have been made to clarify various aspects of the earthquake-induced impact between adjacent structures. A part of these works was devoted to develop different linear and non-linear models to simulate seismic pounding [1]. The non-linear viscoelastic model proposed by Jankowski [2] and a Hertz contact model with nonlinear damping developed by Muthukumar and Desroches [3], for instance, are the results of these researches.

Soil-structure interaction and torsional eccentricity are important factors which may impress seismic response of neighboring buildings. The soil-structure interaction effect arises from transferring seismic waves between adjacent foundations which is called structure-soil-structure interaction, or SSSI. Reviewing the literature shows that one- or two-dimensional models without including torsional response and soil-structure interaction have been mainly utilized to investigate seismic pounding response of adjacent structures. In addition, other studies have been conducted on seismic impact of three-dimensional unsymmetric adjacent structures resting on a rigid base, i.e. excluding SSSI, or symmetrical buildings on flexible soils, where effect of mass eccentricity has been disregarded. Only a small portion of research works has been dedicated to simultaneous modeling of pounding and SSI, with or without torsional coupling. In this regard, the following works can be cited.

Rahman et al. studied the effects of soil flexibility on the seismic responses of adjacent moment frames including planar impact [4]. For this purpose, 6- and 12-story concrete buildings were considered and the underlying soil was modeled with discretized springs and dampers. Results of nonlinear dynamic analyses showed that the intensity of impact was considerably related to the level of soil flexibility.

Mahmoud et al. [5] studied the pounding response of adjacent one-dimensional models of multi-story buildings including SSI. They developed 3-story models on soil springs and dampers and utilized a modified nonlinear viscoelastic pounding element. It was shown that flexibility of soil alters the pattern of impact forces especially in the lower stories where the pounding force could even increase. Naserkhaki et al. [6] investigated the pounding response of one-dimensional adjacent structures on flexible soils. The pounding element was selected to be a linear viscoelastic element and the soil was modeled by spring/damper elements. They concluded that pounding along with SSI could result in larger story responses compared with the response of a similar

* Corresponding author.
E-mail address: farhad@cc.iut.ac.ir (F. Behnamfar).

https://doi.org/10.1016/j.engstruct.2019.05.080
Received 12 January 2019; Received in revised form 17 May 2019; Accepted 25 May 2019
Available online 08 June 2019
0141-0296/ © 2019 Elsevier Ltd. All rights reserved.

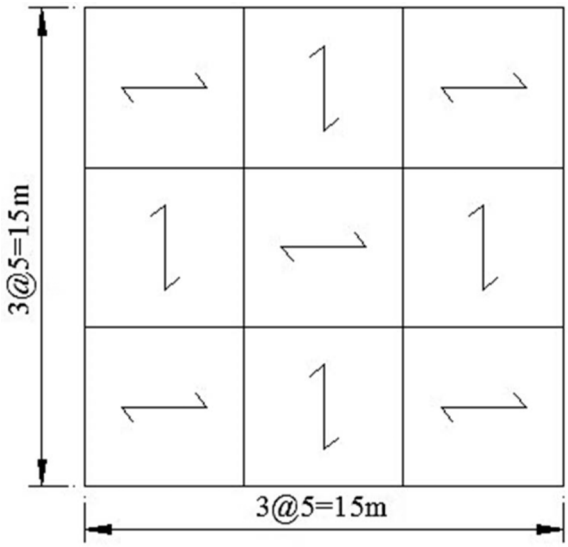

Fig. 1. Plan of the building models.

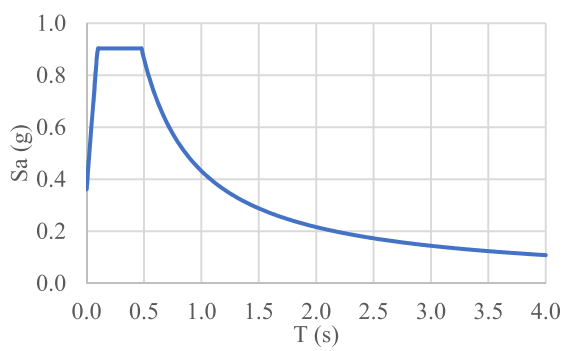

Fig. 2. The utilized design response spectrum.

single structure on rigid base.

Madani et al. [7] studied two-dimensional adjacent buildings resting on flexible bases and explored the effects of pounding. The pounding element in their research consisted of a series of linear viscoelastic contact elements one at each story. Five pairs of buildings were considered at 0, 50, and 100% of the prescribed clear distance required by the reference building code. The underlying soil was modeled by viscoelastic dampers and nonlinear and linear springs in series to model the soil behavior in the near and far domains, respectively. The structures were also modeled as inelastic systems with nonlinearities concentrated at the ends of members. It was concluded that the soil flexibility changed distribution of responses such that it increased the pounding force and nonlinear responses in other stories.

In the study of Ghandil and Aldaikh [8], a linear viscoelastic element was utilized for modeling of pounding. They modeled SSI using the direct method. Value of the clear distance was set according to IBC 2009. It was concluded that a free space three times that of the value recommended by the code was necessary in order to prevent pounding when SSI is taken into account. In addition, extent of damage was wider in the larger building. Kontoni and Farghaly [9] utilized a two-dimensional model to study the seismic impact problem of two adjacent buildings resting on a flexible medium using the direct method. The case of uneven foundations was also studied. Their investigation highlighted the importance of simultaneous pounding and structure-soil-

Table 2
Dimensions of the foundations.

Building	Foundation Type	Length (m)	Width (m)	Thickness (m)
4-story	Strip	15	0.9	0.7
7-story	Strip	15	0.9	1.3
10-story	Mat	15	15	1

Table 3
Fundamental periods of the fixed-base building models.

Building	Fundamental period (sec)
4-story	1.1
7-story	1.96
10-story	2.33

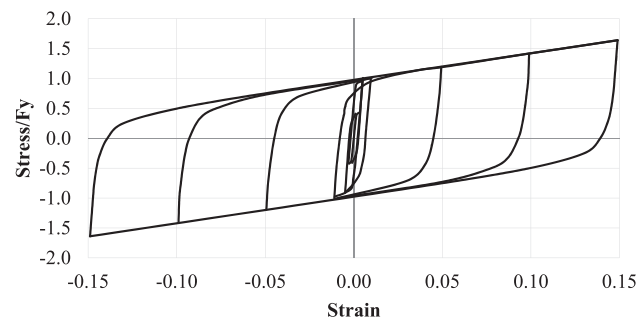

Fig. 3. The stress-strain relation of Steel02 material [15].

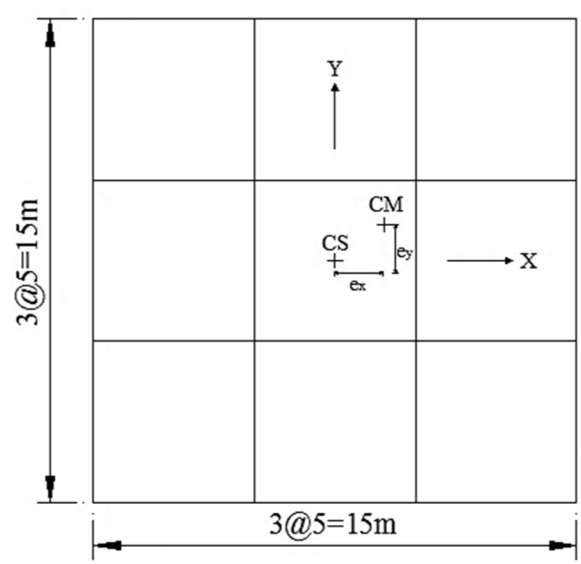

Fig. 4. Displacing the center of mass to simulate torsional eccentricity.

Table 1
The typical sections of the structural members.

Building	Beam sections	Column sections
4-Story	IPE 300 and 330	Box 200 × 17.5 and 260 × 17.5
7-Story	IPE 270, 300 and 360	Box 180 × 17.5, 220 × 17.5, 240 × 17.5 and 260 × 17.5
10-Story	IPE 330, 360 and 400	Box 240 × 17.5, 280 × 17.5, 300 × 17.5 and 340 × 17.5

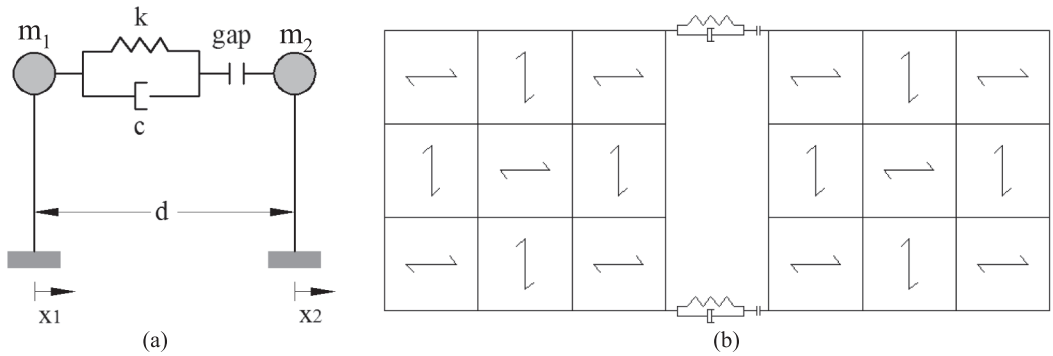

Fig. 5. The linear viscoelastic contact model. (a) Simple analytical model. (b) Locations of the contact (impact) elements in the plan of the adjacent diaphragms.

Table 4
Separation distances calculated for the adjacent buildings.

Width of the separation joint (m)	Adjacent structures
0.19	4, 4
0.25	4, 7
0.18	4, 10
0.33	7, 10
0.38	10, 10

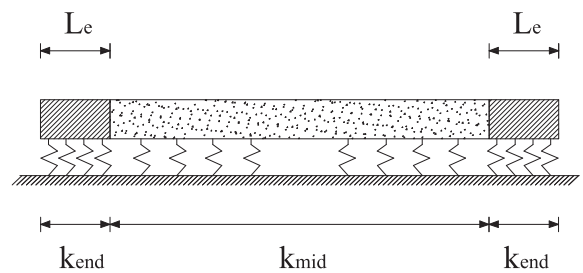

Fig. 8. Distribution of vertical springs for rigid foundations [23].

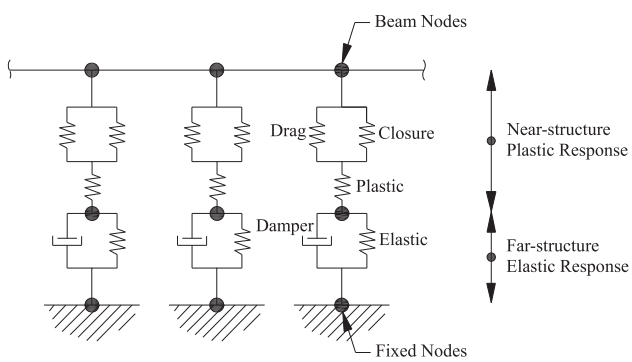

Fig. 6. The nonlinear model of the flexible base [20].

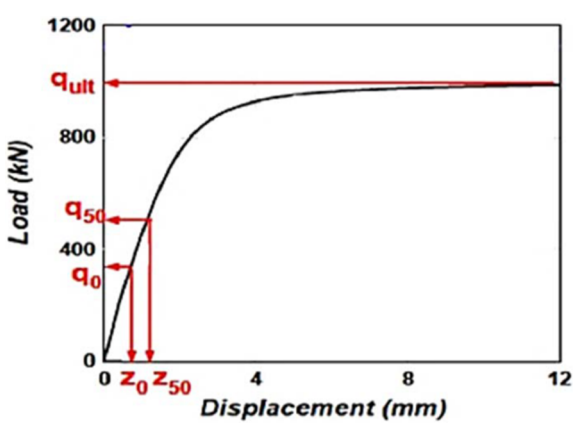

Fig. 7. The Qzsimple model [21].

structure interaction. Fatahi et al. [10] analyzed a three-dimensional model of three similar and in-line 15-story buildings resting on pile groups using Abaqus. The horizontal seismic motion was input in the direction of adjacency. The results exhibited an amplification in the story shear forces due to pounding.

The study of Pawar and Murnal [11] is one of the few studies on the seismic response of adjacent unsymmetric structures on a flexible base. They used concentrated springs to model the flexibility of soil. It was concluded that SSI increased number of impacts and the displacement amplitude but it decreased the pounding force and the story shears.

Review of the aforementioned research tasks confirms the fact that how the research works on pounding response of adjacent structures including torsion and SSI concurrently are rare. As proximity of buildings, torsional response due to at least variation of location of the live load, and flexibility of the underlying soil are most often simultaneously present, a study on concurrent effects of the above conditions seems to be an important need. This is the incentive of the current research where nonlinear pounding of representative adjacent buildings is investigated along with torsional eccentricity of buildings and flexibility of the underlying soil.

Moreover, it is important to note that diaphragms of adjacent buildings can be at the same levels or not. The latter case seems to pose a more critical condition locally where diaphragms of a building collide with the exterior columns of the other. On the other hand, the pounding force is expected to be smaller in this case since the rigid slabs impact the much softer columns. Therefore, the case of identical-level diaphragms should have a stronger effect on the structural responses globally. For this reason, the same case has been selected for this study.

2. Description of the building models

2.1. Buildings geometry and structural system

Three 4, 7, and 10-story steel special moment frame buildings having a same 15 × 15 m plan (shown in Fig. 1) and identical story heights equal to 3.3 m are considered for the purpose of this study. The underlying soil medium is considered to be soft and corresponding to the site class D according to ASCE 7-10 [12] criteria. The buildings are designed assuming a very high seismicity region, residential occupancy and an allowable bearing stress of 1.8 kgf/cm^2 for the foundation. The utilized design response spectrum is illustrated in Fig. 2. It is worth mentioning that just the minimum eccentricity prescribed by the code is

Table 5
The horizontal and vertical stiffness values for the linear springs.

Number of stories	Vertical stiffness (N/m)			Horizontal stiffness in the x-direction (N/m)	Horizontal stiffness in the y-direction (N/m)
	Width of the exterior zone	End stiffness	Middle stiffness		
4	–	–	2.41*G*	12.58*G*	16.1*G*
7	–	–	1.67*G*	14.52*G*	17.94*G*
10	2 m	0.62G	0.252*G*	43.12*G*	43.12*G*

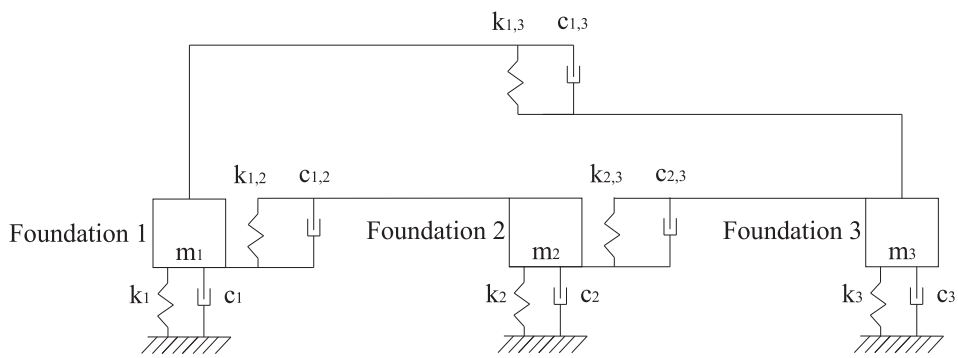

Fig. 9. The discretized foundation-soil-foundation model [24].

Table 6
Coupling stiffness and damping coefficients [24].

Damping factor (ψ)	Stiffness factor (Γ)	Damping (c_{ij})	Stiffness (k_{ij})	Degree of freedom
8.504	$1.614 \times 10^{-0.16257(d/a)}$	$\psi_3 \times \frac{Ga^2}{V_S(1-\upsilon)}$	$\Gamma_3 \times \frac{Ga}{(1-\upsilon)}$	Vertical
13.2875	$3.7561 \times 10^{-0.18995(d/a)}$	$\psi_1 \times \frac{Ga^2}{V_S(2-\upsilon)}$	$\Gamma_1 \times \frac{Ga}{(2-\upsilon)}$	Horizontal
$7.3823 - 6.775Log_{10}(d/a)$	$-(0.96 - 0.88d/a)$	$\psi_{\phi 2} \times \frac{Ga^4}{V_S(1-\upsilon)}$	$\Gamma_{\phi 2} \times \frac{Ga^3}{(1-\upsilon)}$	Rocking

Table 7
Variation of the fundamental period (s) with the clear distance ratio.

Building pair	Fixed-base period	Flexible-base period of the twin building at d = 1	Flexible-base period of the twin building at d = 0.5	Flexible-base period of the twin building at d = 0
4, 4	1.10781	1.12272	1.12269	1.12265
4, 7	1.87636	1.95541	1.95538	1.90130
4, 10	2.27665	2.32972	2.32970	2.31715
7, 10	2.64399	2.34499	2.34478	2.34458
10, 10	2.29666	2.34847	2.34842	2.33938

Table 8
Ground motion selection criteria.

Magnitude	Distance (km)	Shear wave velocity(V_{S30})
$6 \le M \le 7.5$	$20 \le D \le 50$	Consistent with the soil type D

considered in design stage and torsional eccentricity is simulated by dislocating the center of mass of the stories in the nonlinear analysis phase. The structural members and the foundations are designed according to ANSI/AISC 360-10 [13] and ACI 318-14 [14], respectively. Tables 1 and 2 summarize the design sections and foundations characteristics of the buildings. The fundamental periods of the fixed-base building models are listed in Table 3.

Five pairs of adjacent buildings including (4, 4), (4, 7), (4, 10), (7, 10), and (10, 10) are studied where the numbers refer to the number of stories. For example, a (7, 10) case refers to a 7-story building adjacent to a 10-story one.

2.2. Nonlinear modeling of structural elements

The open source software Open System for Earthquake Engineering Simulation (OpenSees) [15] is used to model and analyze the considered building pairs of this study. Concentrated plastic hinges are assigned to the structural members (i.e., beams and columns) in order to model their nonlinear behavior in bending. The nonlinear moment-rotation relation of plastic hinges is calculated by analyzing their corresponding fiber sections considering nonlinear behavior of steel. An OpenSees constitutive model named steel02 is chosen to simulate nonlinear stress-strain relation of steel (Fig. 3). This material model is more accurate and has superior convergence rate compared with other alternatives.

Table 9
Characteristics of the records selected and scaled for each building pair.

Event	RSN number	Year	Unscaled PGA (g)		Scale factor	Building pair
			H1	H2		
San Fernando	57	1971	0.29	0.27	1.54	(4,4), (4,7), (4,10)
San Fernando	78	1971	0.11	0.10	1.81	(7,10), (10,10)
Irpinia Italy-01	286	1980	0.10	0.08	1.44	All of the Building Pairs
Loma Prieta	755	1989	0.15	0.49	1.59	All of the Building Pairs
Chi-Chi Taiwan	1484	1999	0.25	0.21	1.43	All of the Building Pairs
Duzce Turkey	1616	1999	0.03	0.04	1.43	All of the Building Pairs
Cape Mendocino	3747	1992	0.14	0.18	1.44	(7,10), (10,10)
Cape Mendocino	3750	1992	0.25	0.26	1.45	(4,4), (4,7), (4,10)
Landers	3753	1992	0.22	0.20	1.43	(4,4)
Landers	3757	1992	0.14	0.14	1.43	(4,7), (4,10), (7,10), (10,10)
Niigata Japan	4214	2004	0.20	0.23	1.53	All of the Building Pairs
Chuetsu-oki	4868	2007	0.32	0.36	1.44	(4,4)
Chuetsu-oki	5265	2007	0.46	0.34	1.53	(4,7), (4,10), (7,10), (10,10)
Iwate	5663	2008	0.50	0.66	1.79	All of the Building Pairs
Darfield New Zealand	6971	2010	0.16	0.16	1.44	All of the Building Pairs

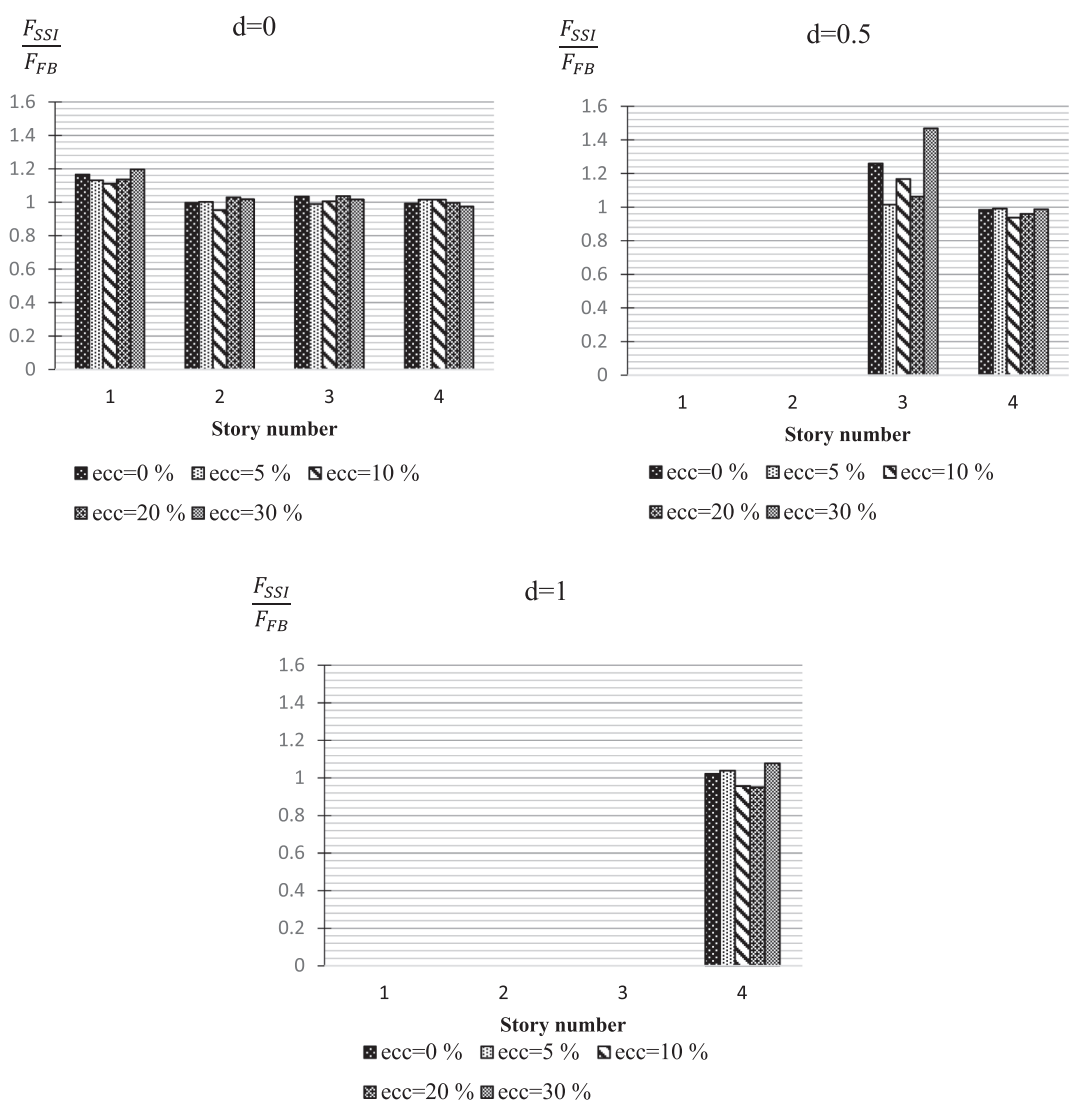

Fig. 10. Values of the pounding force with SSI normalized to those without SSI.

Table 10
Maximum ratio of the SSI pounding force to the one without SSI (PF) and the associated parameters for different cases.

Building pair	d	Ecc., %	Story	PF
4, 4	0	5	1	1.26
4, 7	1	20	4	1.2
4, 10	0.5	30	3	1.46
7, 10	0.5	0	6	1.7
10, 10	1	30	6	1.83

2.3. Modeling torsional eccentricity

As mentioned before, the buildings have been designed considering the minimum eccentricity prescribed by the code. The location of the center of mass is shifted afterwards in order to model the torsional response and investigate the effects of eccentricity on the earthquake-induced pounding between adjacent buildings, as can be seen in Fig. 4. The eccentricity ratios in both horizontal directions (i.e. x and y) are assumed to be identical and occur concurrently in order to limit the number of case studies and eventually five different eccentricity ratios including 0, 5, 10, 20, and 30% are assumed for covering various common and rare (i.e., 30%) cases.

3. The impact element

Modeling the impact between two neighboring structures is one of the challenges in earthquake-induced pounding studies. Several models have been developed including elastic, viscoelastic, plastic and Hertz models [2,3]. The linear viscoelastic model is selected out of the existing pounding models. This model is simple enough and can simulate energy dissipation in impact, which is an important phenomenon in pounding modeling. The linear viscoelastic model is a widely used model and Fig. 5a demonstrates different elements of this model.

As observed in Fig. 5a, the linear viscoelastic model consists of an impact compressional spring, a dashpot and a gap element. The impact spring behaves linearly and its stiffness should be determined based on experimental data. As full-scale experiments on colliding concrete diaphragms are rare, the spring coefficient is selected solely based on computational needs. This spring should be stiff enough to prevent the colliding diaphragms from penetrating each other. Theoretically, this condition results in the spring coefficient to be infinity but it is computationally sufficient to increase the coefficient as far as where it has no further effect on the structural responses.

According to Muthukumar and Desroches [3] and Madani et al. [7] studies, values ranging from 1×10^9 to 1×10^{11} N/m can be used for the spring coefficient of the pounding element between typical building diaphragms. It has been also shown that changing the magnitude of spring stiffness by one order does not alter the structural response sensibly [16,17]. The sensitivity analysis in the current study also shows that assuming stiffness values larger than 1×10^9 N/m is sufficient for the pounding analysis of the considered models.

The linear viscoelastic model is able to simulate energy dissipation by using a dashpot element. The damping coefficient of this dashpot can be calculated by Eqs. (1) and (2) [18,19]:

$$c = 2\xi\sqrt{k\left(\frac{m_1 m_2}{m_1 + m_2}\right)} \tag{1}$$

$$\xi = -\frac{\ln(e)}{\sqrt{\pi^2 + (\ln(e))^2}} \tag{2}$$

In these equations, ξ stands for damping ratio, m_1 and m_2 are the adjacent masses, k is the impact spring stiffness and e refers to the coefficient of restitution. The coefficient of restitution is defined as the ratio of the relative velocity of two colliding bodies after impact to their initial relative velocity. Hence, the value of $e = 1.0$ is corresponding to no energy dissipation. Previous researches adopted values range from 0.6 to 0.7 for pounding modeling. In the current study, the coefficient of restitution is assumed to be equal to 0.65.

The linear viscoelastic impact model utilizes a gap to account for the clear distance between adjacent impacting bodies. Value of the gap is calculated with regard to ASCE 7-10 [12]. According to ASCE 7-10 [12] regulations, the separation distance can be determined by Eq. (3):

$$\delta_{MT} = \sqrt{(\delta_{M1})^2 + (\delta_{M2})^2} \tag{3}$$

where δ_{MT} is the minimum required separation distance between adjacent structures and δ_{M1} and δ_{M2} refer to the maximum nonlinear displacements of the buildings at their adjacent edges. δ_{Mi} can be calculated using the following equation [12]:

$$\delta_{Mi} = \frac{C_d \delta_{max}}{I_e} \tag{4}$$

where C_d is the deflection amplification factor, δ_{max} refers to the maximum linear displacement calculated using a design spectrum and I_e is the importance factor. Using Eqs. (3) and (4) with $C_d = 5.5$ for the special steel moment-resisting frame system and $I_e = 1.0$ for residential occupancy, the minimum clear distance required by the code can be calculated for the considered pairs of buildings, as summarized in Table 4.

In order to investigate the influence of separation distance on the seismic responses, the clear distance between adjacent buildings is taken equal to 0, 50 and 100% of the Table 4 distances. The reasons for considering cases violating the code are twofold. First, there are many existing buildings built in the past where the current minimum separation distance was not observed. Second, it is intended to verify that how important it will be if the minimum distance is not provided. It is studied by accounting for the important factors including the torsional response and soil-structure interaction.

It should be noted that the impact does not occur uniformly along adjacent edges of the torsional buildings and it can happen just at one corner. Therefore, at each story, an impact element is assigned to each corner of the adjacent edges to simulate the pounding more accurately, as shown in Fig. 5b.

4. Soil-structure interaction modeling

As mentioned in Section 2.1, a soft soil medium corresponding to the site class D [12] is considered to be underlying the studied structures. Characteristics of this medium are assumed to be: cohesion = 3 KN/m^2, friction angle = 35°, specific weight = 19 KN/m^3, shear wave velocity = 200 m/s^2, and damping ratio = 0.05 The other properties of the soil medium are described in the following.

4.1. The SSI model

A model of beam on nonlinear Winkler springs and viscous dampers is used for nonlinear modeling of SSI. It is schematically shown in Fig. 6.

The above model consists of nonlinear springs representing the nonlinear behavior of soil just below the foundations, and linear springs and dashpots simulating the flexibility of the underlying soil and the radiation damping. The foundation itself is discretized at its common nodes with the plastic soil springs, being spaced at about 25 cm.

Nonlinearity of the soil springs is introduced using the Qzsimple and

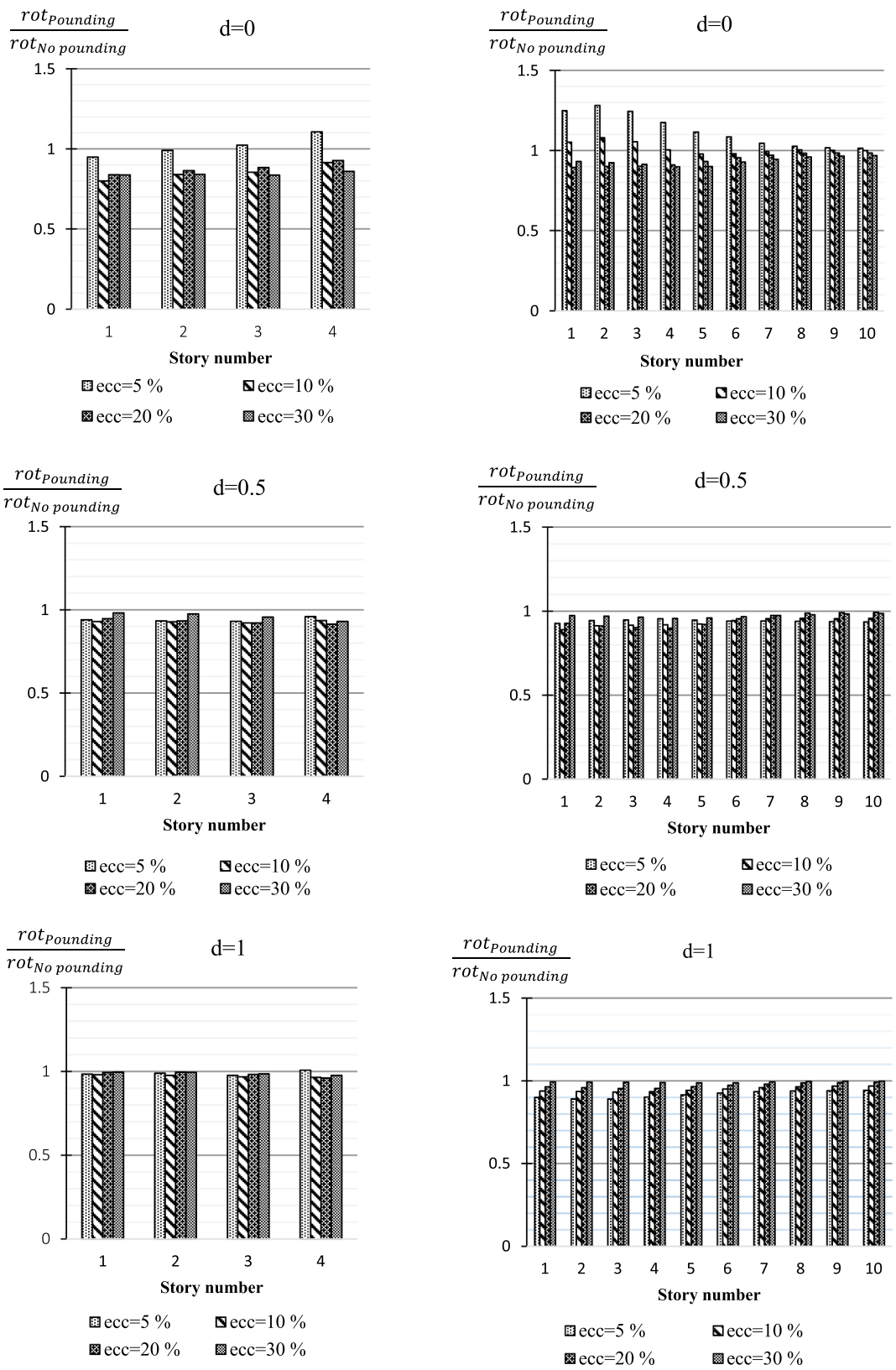

Fig. 11. Values of the maximum horizontal rotation of each story normalized to the corresponding value of the single building.

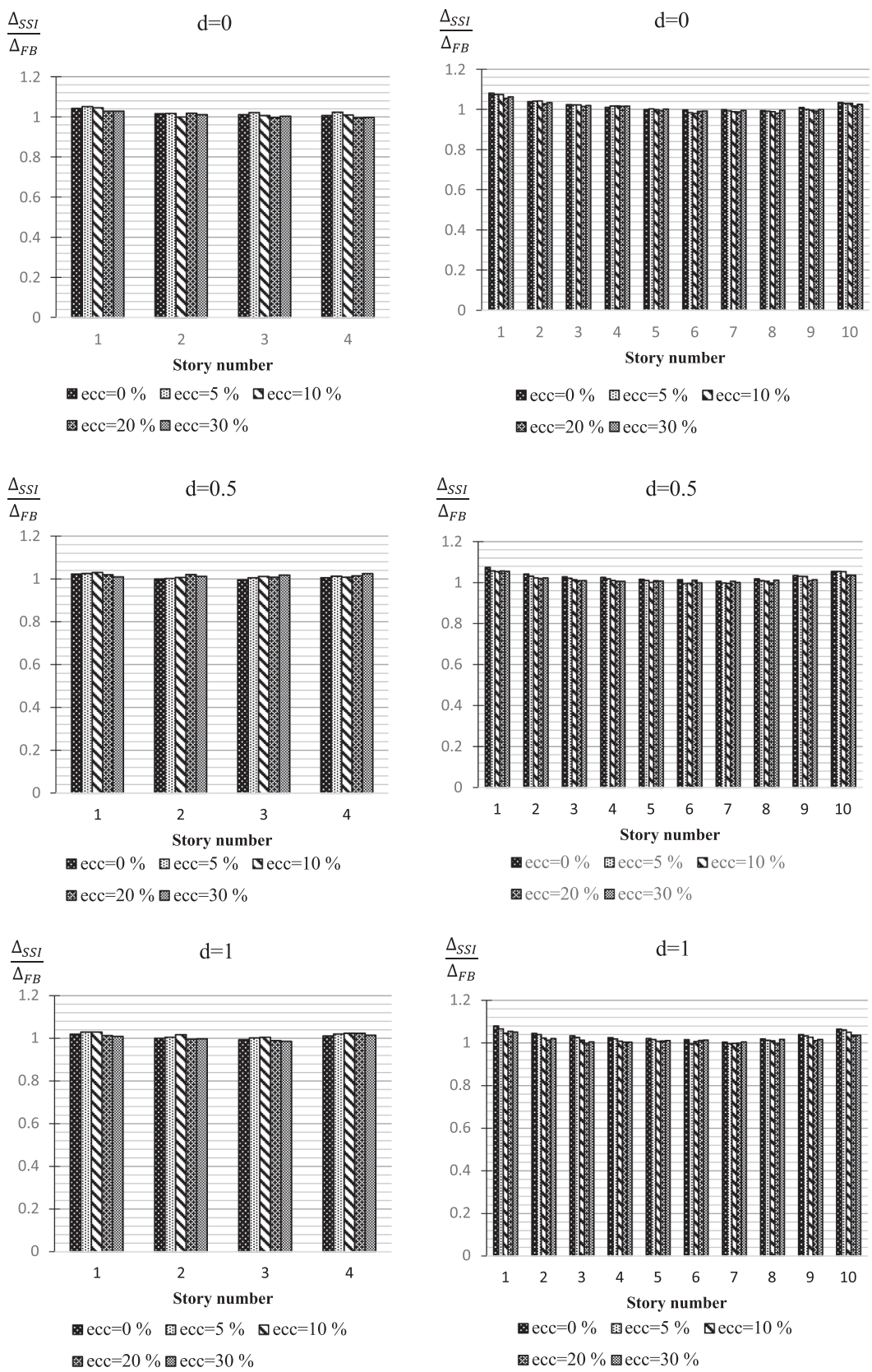

Fig. 12. Ratios of the story drifts with SSI to those without SSI for the (4, 10) building pair.

Table 11
Maximum percentages of decrease and increase of the story drift ratios (DRD and DRI, respectively) for the building pairs, normalized to their fixed-base associates.

	Shorter building			Taller building			Shorter building			Taller building		
	Ecc (%)	Story	DRD	Ecc (%)	Story	DRD	Ecc (%)	Story	DRI	Ecc (%)	Story	DRI
4, 4	10	3	12	–	–	–	10	1	3	–	–	–
4, 7	30	3	3	30	6	3	5	1	3	20	1	1.7
4, 10	30	3	2	10	6	2	5	1	5	0	1	8
7, 10	30	6	1.5	20	6	1.3	0	7	3	0	10	7
10, 10	20	5	2	–	–	–	0	10	10	–	–	–

Table 12
Maximum percentages of reduction (DR) and increase (DI) of the drift ductility demands of the building pairs with SSI normalized to the corresponding cases without SSI.

Building pair	Shorter building			Taller building			Shorter building			Taller building		
	Ecc(%)	Story	DR	Ecc(%)	Story	DR	Ecc(%)	Story	DI	Ecc(%)	Story	DI
4, 4	10	3	13	–	–	–	10	1	4	–	–	–
4, 7	30	3	4	30	6	2.5	5	1	3	20	1	1.6
4, 10	30	3	2	10	6	2	5	1	5	0	1	9
7, 10	30	6	2	20	6	1.5	0	7	3.5	0	10	7
10, 10	20	5	1.5	–	–	–	0	10	11	–	–	–

Tzsimple soil models in the vertical and horizontal directions, respectively. The mentioned models have been developed by Boulanger [21] and Harden et al. [20]. In both of the mentioned soil models, the load-displacement curve represents an elastoplastic behavior. It is shown for instance for the Qzsimple model in Fig. 7.

Parameters of the Qzsimple are qzType, q_{ult}, z_{50}, suction, and c. "qztype" refers to the soil type being sand or clay, that is taken to be sand in this study. "q_{ult}" is the bearing capacity of foundation. In this research, it is calculated using the theory of Meyerhoff [22] to be 1.22, 1.44 and 5.33 kgf/cm^2 for the 4, 7 and 10-story buildings, respectively. "z_{50}" is the foundation deformation at 50% of the bearing capacity. It is calculated using Eq. (5):

$$z_{50} = \frac{1.3q_{ult}}{k_z} \quad \text{(For the Qzsimple material)} \tag{5}$$

where k_z is the vertical stiffness of soil per unit length to be described later. "Suction" is the tensile capacity of foundation taken to be zero, and c is coefficient of the radiation damping to be mentioned afterwards.

The Tzsimple material, introduced by tzType, is taken to be sand. z_{50} is calculated for this material using Eq. (6):

$$z_{50} = \frac{2.05t_{ult}}{k} \quad \text{(For the Tzsimple material)} \tag{6}$$

where k is the horizontal stiffness of foundation per unit length (to be calculated in the following), and t_{ult}, the horizontal capacity of foundation, is determined using Eq. (7):

$$t_{ult} = W_g tan(\delta) + A_b C \tag{7}$$

where W_g is the vertical load, δ is the friction angle between the soil and foundation, A_b is the plan area of foundation, and C is the cohesion factor of soil. t_{ult} is calculated to be 3.4, 6.2, and 9.66 MN for the 4, 7, and 10-story buildings respectively. Values of the distributed vertical and horizontal stiffnesses of soil are needed for the model of Fig. 7. According to ASCE41-13 [23], before being able to calculate the above values, it must be determined whether the foundations are rigid or flexible with regard to the underlying soil using Eqs. (8a) and (8b) for strip and mat (or single) foundations, respectively:

$$\frac{E_f I_f}{L^4} > \frac{2}{3} K_{sv} B \tag{8a}$$

$$4K_{sv} \sum_{m=1}^{5} \sum_{n=1}^{5} \frac{sin^2(\frac{m\pi}{2}) sin^2(\frac{n\pi}{2})}{\pi^4 D_f \left(\frac{m^2}{L^2} + \frac{n^2}{L^2}\right) + K_{sv}} < 0.03 \tag{8b}$$

The foundations are taken to be rigid if the above inequalities hold. In the above relations, I_f, E_f, L, and B are the moment of inertia of the cross section, modulus of elasticity, length and width of the foundation, respectively, and K_{sv} and D_f are:

$$K_{sv} = \frac{1.3G_o}{B(1-\upsilon)} \tag{9a}$$

$$D_f = \frac{E_f t^3}{12(1-\upsilon_f)^2} \tag{9b}$$

where υ_f and t are the Poisson's ratio and thickness of foundation. Then, if the foundations are flexible, their vertical stiffness per unit area is calculated using Eq. (9a) [23]. Otherwise, a distribution of vertical springs is considered according to Fig. 8, consisting of softer springs in the middle and stiffer ones elsewhere.

Length of the end regions, L_e, in Fig. 8 is equal to:

$$L_e = 0.5L - L\left[\frac{1}{8}(1 - C^k_{R-V})\right]^{\frac{1}{3}} \tag{10a}$$

$$C^k_{R-V} = \frac{K_{\theta y} - \frac{K_z}{A} I_y}{K_{\theta y}} \tag{10b}$$

where $K_{\theta y}$ and K_z are the foundation stiffnesses in rotation about the horizontal axis, y, perpendicular to the direction of lateral motion, and in the vertical direction, respectively. A and I_y are the plan area and the

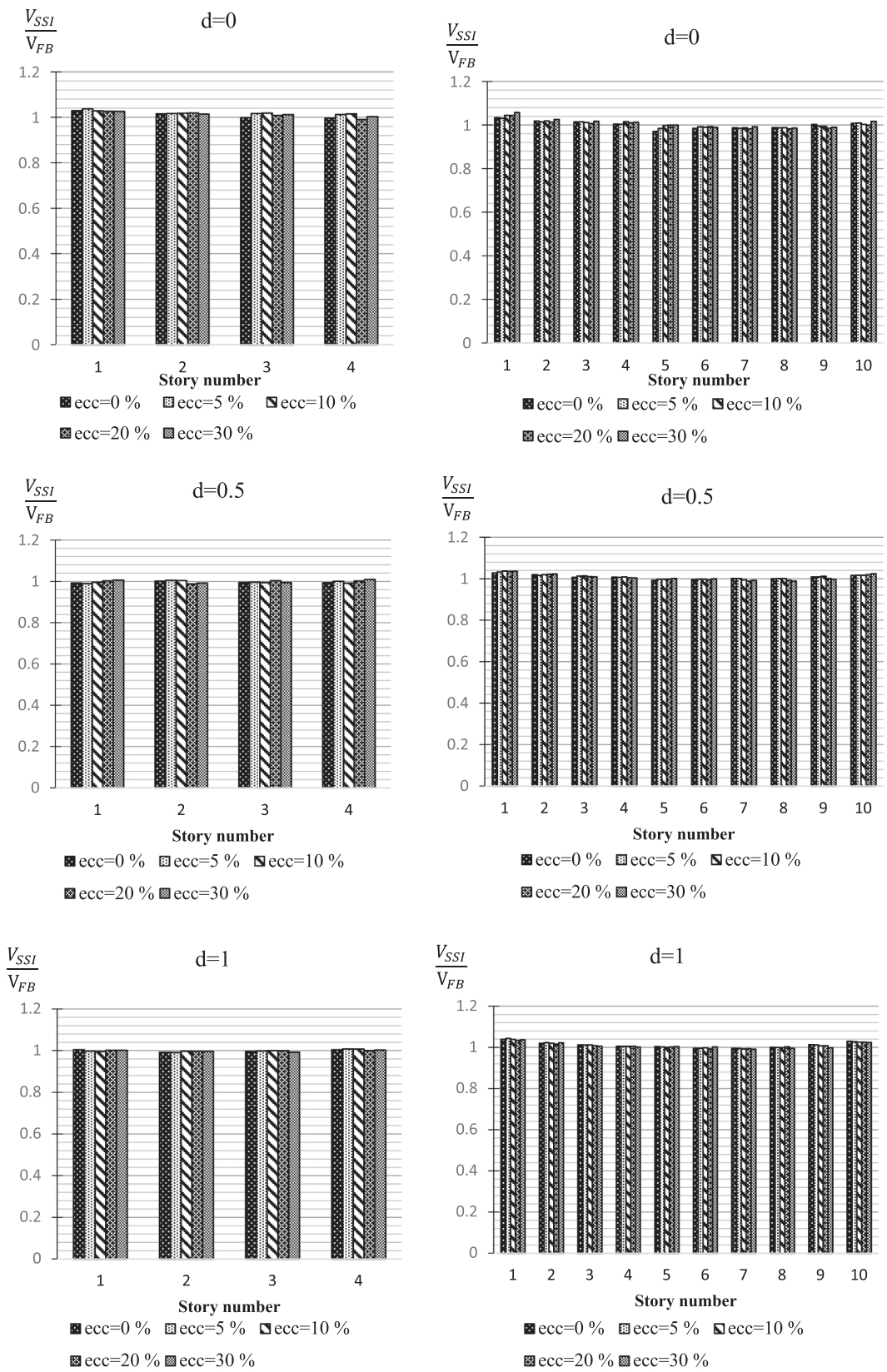

Fig. 13. Distribution of the story shears with SSI normalized to the associated values without SSI for the (4, 10) building pair.

Table 13
Maximum percentages of decrease and increase of the story shears (SD and SI, respectively) of the building pairs normalized to their fixed-base associates.

Building pair	Shorter building			Taller building			Shorter building			Taller building		
	Ecc (%)	Story	SD	Ecc (%)	Story	SD	Ecc (%)	Story	SI	Ecc (%)	Story	SI
4, 4	10	4	4	–	–	–	20	1	3			
4, 7	20	4	3	30	7	3	0	1	2	0	1	1.4
4, 10	20	2	1.2	0	5	3	5	1	4	30	1	6
7, 10	30	7	3	5	8	2	20	1	3	30	1	4
10, 10	30	9	3	–	–	–	0	10	7	–	–	–

moment of inertia of foundation about the y-axis, respectively.

The vertical soil springs in the middle, K_{mid}, and end regions, K_{end}, of Fig. 8 are [20]:

$$K_{mid} = \frac{K_z}{BL} \tag{11a}$$

$$K_{end} = aK_{mid} + \frac{K_{\hat{\theta}y}}{I_y} C^k_{R-V} \tag{11b}$$

The radiation damping of soil in the vertical direction, C_z is calculated using Eq. (12) [20]:

$$C_z = \rho V_{LA} A_b C_z \tag{12a}$$

$$V_{LA} = \frac{3.4}{\pi(1-\upsilon)} V_s \tag{12b}$$

where ρ, V_s, and υ are the mass density, shear wave velocity and Poissons's ratio of soil, respectively, and C_z is a damping coefficient varying between 1 and 2 as a function of the governing frequency of excitation and L/B. The overall stiffness values of rigid foundations are given by ASCE41-13 [23] or Harden et al. [20]. Values of the calculated linear spring stiffnesses for the foundations are given in Table 5.

The parameter G in Table 5 is the shear modulus of soil for large strains. It is varied as a function of soil type and the effective peak acceleration at the ground surface [23]. As mentioned in Section 2.1, a very high seismicity region has been considered for this study. Fig. 2 shows that the effective peak acceleration at the ground surface (normalized to the acceleration of gravity), i.e. value of the design spectrum at T = 0, is 0.35. For a soil type D and such a peak acceleration, value of G is calculated using the corresponding table in ASCE 41-13 [23], to be 55% of G_O where $G_0 = \rho V_s^2$ is the shear modulus of soil for small strains.

4.2. The SSSI model

Transfer of the vibration energy between the adjacent structures occurs through the underlying soil in addition to pounding. Such a phenomenon is called structure-soil-structure interaction (SSSI). Mulliken and Karabalis [24] derived formulas for springs and dampers connecting adjacent foundations for a discretized simulation of cross-interaction between such bodies through the soil, based on regression between the results of many sample finite and boundary element calculations. Their lumped parameter model is suitable for the purposes of this study and used for the related computations. Fig. 9 shows the mentioned set of springs and dampers between the individual foundations. The spring stiffnesses and damping coefficients are given in Table 6. In this table, a equals half dimension of the equivalent rectangular footing and d is the clear distance between the adjacent foundations. Two different approaches are possible for the SSSI modeling. In the first one, the cross interaction is accounted only between the columns located at the side of each building adjacent to the other one. This is especially appropriate when the foundations are of single or strip types. When the foundation system of both buildings is a single mat foundation, a second approach is also possible. Here the cross interaction is considered between the whole body of the foundations. Since various cases of the adjacent foundation types are considered in this study, the first approach seems to be more rational. Here, dimensions of the foundation area shared by each of the columns of the closest row to the adjacent building are calculated and used with Table 6 to calculate the cross-interaction springs and dampers between the closest rows of the side columns of the adjacent buildings.

Using the above modeling procedure, the fundamental periods of the 4, 7, and 10-story are calculated as shown in Table 7. It is seen that the fundamental period decreases in smaller clear distances. This is in compliance with previous literature [7]. In addition, the fundamental period has an asymptotic variation with the clear distance that is physically true.

5. The ground motions

A suit of 56 consistent ground motions is selected from the PEER Strong Motion database regarding Table 8 criteria. The records are scaled based on ASCE 7-10 [12] method and the records having scale factors closest to unity are chosen for performing the nonlinear response history analyses. The SRSS response spectrum of each pair of the selected earthquake record components is calculated and then the average of the SRSS spectra is scaled in order to calculate a unique scale factor for each pair of horizontal earthquake components. This procedure results in 11 pairs of horizontal ground motions for each building pair. Table 9 summarizes the characteristics of these ground motion pairs. The RSN quantity in this table refers to the Record Serial Number in the PEER database.

6. Nonlinear time history analyses results

6.1. Introduction

In this section, the analyses are performed on both the fixed-base and flexible-base models in order to evaluate the effects of SSI on the pounding response of the torsional buildings in comparison to when SSI is not taken into account. Totally 150 adjacent building models are created considering 5 building pairs and 5 eccentricity ratios (i.e. 0, 5, 10, 20 and 30%) along with 3 clear distance ratios (i.e. 0, 50 and 100%) and 2 base conditions (i.e. with and without SSI). These models are analyzed under 11 ground motion pairs, and hence, 1650 nonlinear time history analyses are performed in this study. The maximum responses of each model under each earthquake excitation are recorded and the average of the maximum values is reported as the representative response value. Finally, the results obtained from flexible-base models are normalized to the associated ones for a similar fixed-base building in the corresponding pair of buildings in order to evaluate

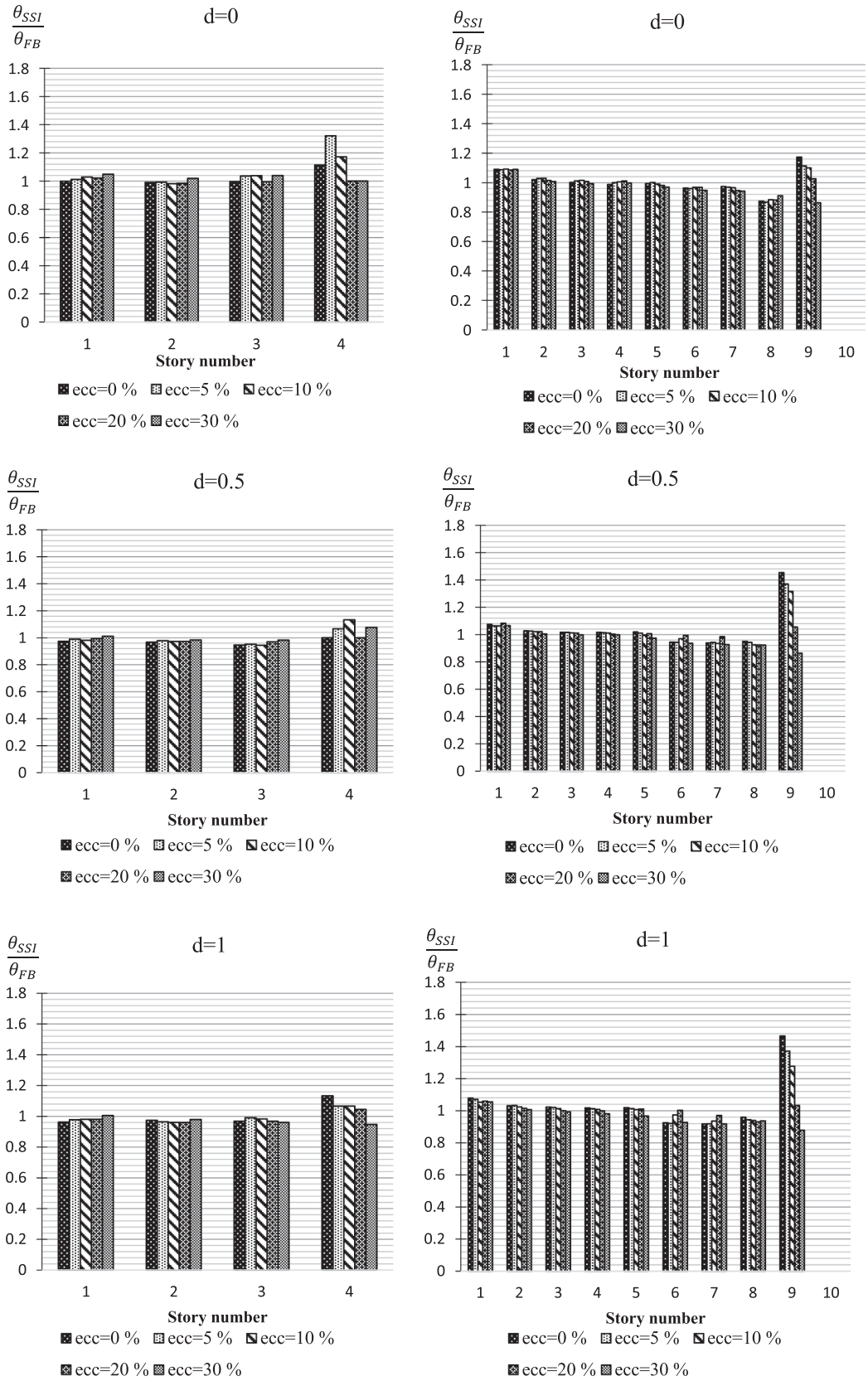

Fig. 14. The resultant PHR's with SSI normalized to those without SSI for the (4, 10) building pair.

Table 14
The averaged maximum lateral displacement at the roof of the 10-story building due to only rotation of its foundation within all eccentricities for different clear distances and the corresponding residual roof displacements (cm).

Building pair	Rot. roof lateral displacement			Rot. roof residual displacement		
	d = 0	d = 0.5	d = 1	d = 0	d = 0.5	d = 1
4, 10	0.61	0.60	0.59	0.044	0.043	0.052
7, 10	1.21	1.20	1.20	0.178	0.173	0.169
10, 10	0.86	0.87	0.87	0.004	0.003	0.003

SSI and SSSI influences. The results are presented as pounding force, drift, ductility ratio, shear force, and the absolute sum of the plastic hinge rotations of each story. Because of the large volume of results, it is not possible to present the complete set here. Thus, for the sake of brevity, only the detailed set of responses for (4, 10) pair of the buildings is presented and just the tabulated results are shown for other building pairs. Further details along with the comprehensive results for all of the building pairs can be found in reference [25].

6.2. The pounding force and horizontal rotation of stories

Values of the pounding force with SSI (F_{SSI}) normalized to those of the fixed-base cases (F_{FB}) are shown in Fig. 10. F_{FB} changes from zero to 1505, 3480, and 5372 kN at the first, second, and third stories, and from 117 to 6867 kN at the fourth story within all eccentricity values.

As observed, for no torsion (ecc = 0%), the maximum ratio of the pounding force at different stories varies from 1 to 1.2 and from 1 to 1.3 for d = 0 and d = 0.5, respectively and it is about unity for d = 1. This is well compared with Ref. [7] where similar values have been reported.

It is seen that for each value of the clear distance, there are stories where for some of the values of the eccentricity ratio, SSI increases the pounding force. The highest increase is about 50%. By increasing the clear distance, SSI exhibits an increasing effect on the pounding force only at the lowest story where pounding happens. The most severe case belongs to a clear distance set as the half of the code value. In this case the lowest story under impact is the third story. Here SSI increases the impact force by about 30 and 50% for the eccentricity ratios of 0 and 30%, respectively. This is a direct result of increase of the relative lateral displacements at the lower stories due to SSI as shown in the next section. Table 10 shows the maximum ratio of the pounding force with SSI to the one for the fixed-base case and its associated parameters for different cases. Moreover, it is observed that pounding may occur even at the code prescribed clear distance. The influence of the eccentricity ratio is not uniform and the pounding force may be increased or decreased by increasing this parameter. However, the maximum pounding force ratios belong to the models having the largest eccentricity ratio (i.e. 30%) in most of the cases. This is the consequence of the increased lateral displacements at larger eccentricity ratios.

It is interesting to see how the pounding force affects the horizontal rotation of stories, i.e., rotation about the vertical axis. Fig. 11 shows the averaged maximum rotation of each story normalized to the corresponding value of the single building. It is seen that pounding is strong enough to affect the horizontal rotation considerably only at d = 0. In such a case, for the shorter building, pounding results in up to 10% lowering of the rotation at larger eccentricities. The exception is at the smallest eccentricity where pounding can amplify the rotation of the upper stories to the same value. Overall, the rotational response is somewhat larger at the upper stories of the shorter building and lower stories of the taller building. In the taller buildings having smaller eccentricities, pounding amplifies the rotation in the stories adjacent to the shorter building, up to 30%. Torsional response of the upper stories is less affected by pounding at such a distance.

6.3. The story drifts and ductility demands

The story drifts with SSI normalized to those without SSI are shown in Fig. 12. The maximum story drift ratio within all eccentricity values without SSI for the 4-story building is 1.01, 1.09, and 1.16% for d = 0, 0.5, and 1, respectively. The corresponding values for the 10-story building are 1.42, 1.42, and 1.44%, respectively.

As observed, independent of the clear distance and value of the eccentricity ratio, the first story drift increases with an almost constant value of about 8%. Therefore, only SSI can be responsible for this phenomenon. In other words, SSI is observed to increase the lateral drifts of the lower stories by relaxation of the boundary condition at the base. The results show that the seismic impact has no significant effect on the drift response of the intermediate stories, but it alters the response of the taller building's upper stories. This can be related to the rotational component of the foundation displacement, which increases the displacement at the upper stories. The eccentricity ratio does not significantly change the overall drift response of story.

Similar events are observed for other building pairs too. Table 11 shows the maximum increments and decrements of the story drifts for the studied building pairs. It can be seen that in the most critical case, SSI increases the drift ratio of the studied buildings up to 10%. The maximum variation belongs to the 10-story building at its top and bottom stories.

The story drifts should be distinguished from the total lateral displacements. SSI mostly increases the lateral displacements because of a nearly rigid rotational motion of foundation in taller buildings. Therefore, it has a small effect on the story drifts. However, as shown in Section 6.5, in combination with torsion and pounding it can considerably change the plastic hinge rotations and nonlinear behavior of a building. Therefore, it is not the overall story responses (drifts) that makes a good basis for evaluation of SSI effects, it should be sought within the local amplification of nonlinear behavior as plastic hinge rotations, i.e. point-to-point seismic damage.

The maximum variations of the ductility demands, i.e. ratio of the maximum displacement to the yield displacement, corresponding to the story drifts of each building with SSI with respect to the corresponding values of the similar cases without SSI, are shown in Table 12.

As seen in Table 12, the trends are similar to Table 11, as expected. The ductility demand ratios are more or less equal to the drift ratios. However, variations of the drift and drift ductility demands themselves are not directly representative of the extent of nonlinear response of a story. It should be investigated in conjunction with variation of the resultant plastic hinge rotations in each story (see Section 6.5).

6.4. The story shears

Values of the story shears with SSI normalized to the ones without SSI are shown in Fig. 13. The maximum base shear within all eccentricity values, normalized to the seismic weight of the building, without SSI for the 4-story building is 17.39, 19.83, and 19.36% for d = 0, 0.5, and 1, respectively. The corresponding values for the 10-story building are 9.96, 9.27, and 9.21%, respectively.

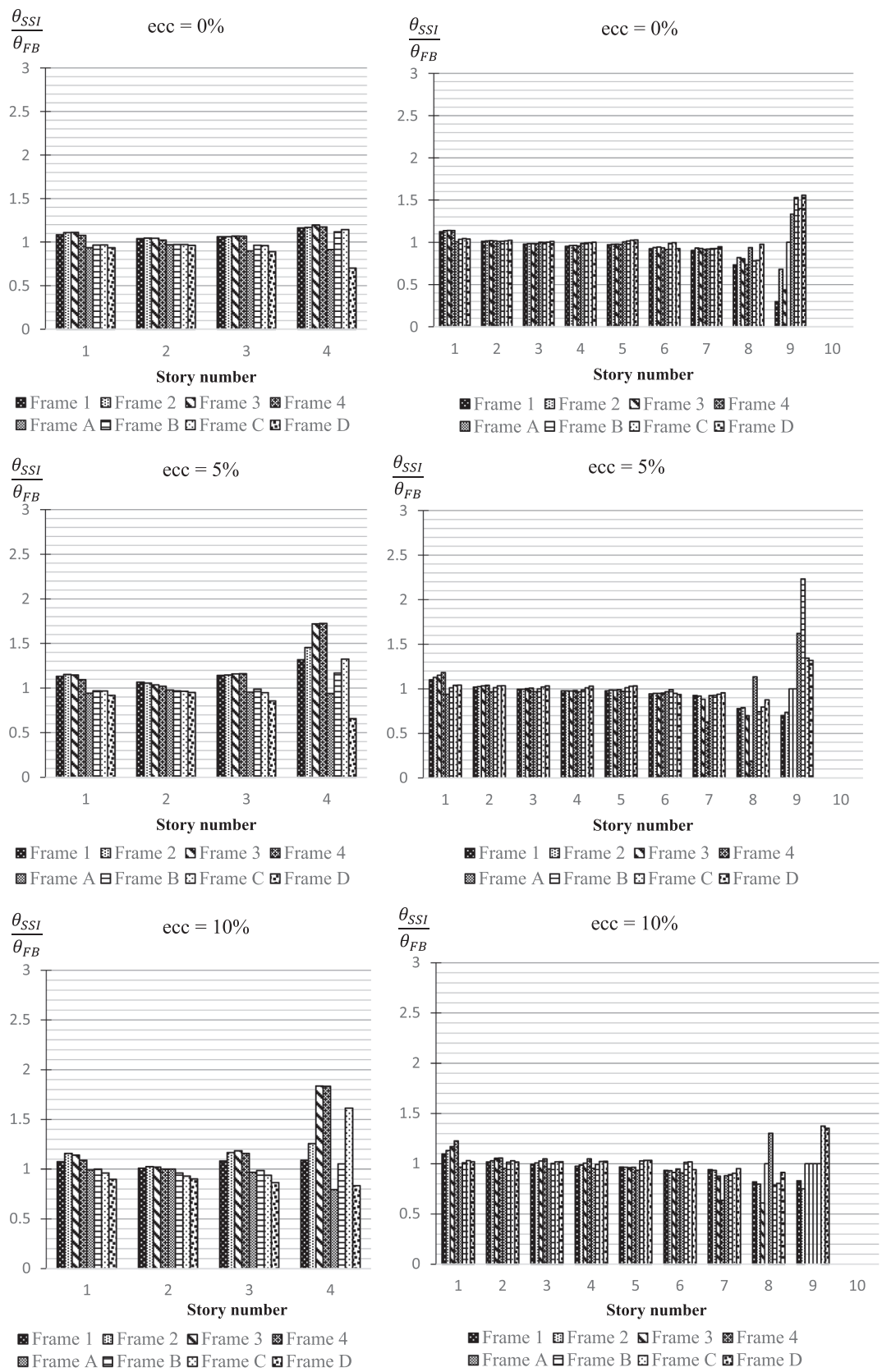

Fig. 15. The PHR ratios for each frame of the (4, 10) building pair with SSI normalized to those of similar frames without SSI for a clear distance ratio of zero.

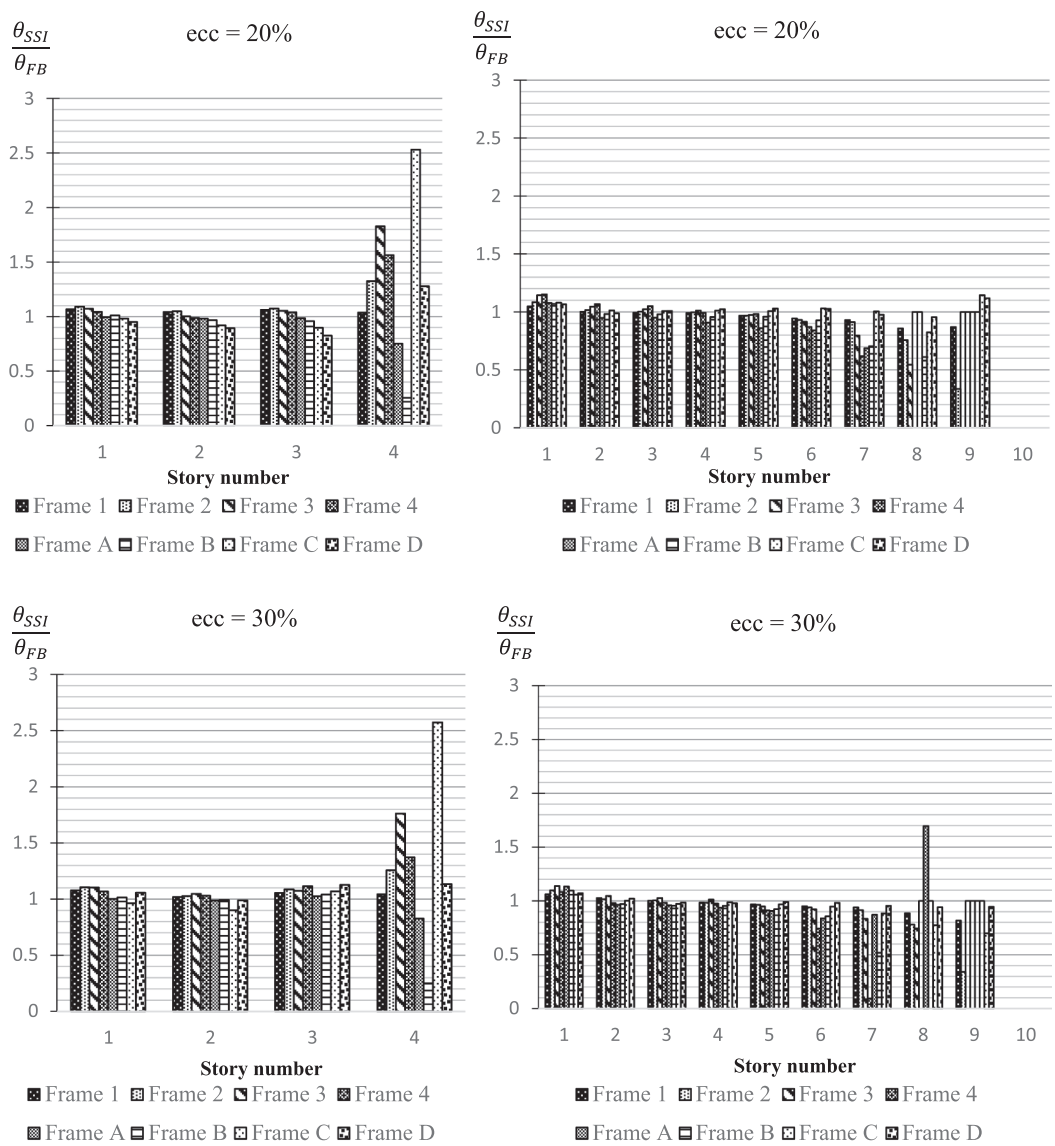

Fig. 15. (*continued*)

Maximum variation of the story shears of the shorter building corresponds to the first story at no clear distance. This case belongs exactly to when the largest increases was observed in the pounding force (see Fig. 10). Therefore, same is the reason for the larger first story shear. In the taller building, the story shear increases up to 6% in the lower and to 3% in the upper stories. It makes almost no change at the intermediate floors. Values very similar to the above results have been reported in Ref. [7] for ecc = 0%. The larger pounding force of the first story can be responsible for the larger story shear at this location. On the other hand, the rotational component of the foundation motion should be the reason for larger accelerations and thus story shears at the upper stories. The diagrams illustrated in Fig. 13 show that the story shear is not significantly affected by the eccentricity ratio.

Table 13 shows the maximum variations of the story shears for the studied building pairs. It is seen that considering simultaneous effects of the torsional response and SSI can alter the story shear of the studied buildings up to 6% in the case of (4, 10) building pair while it is about 3% for other cases.

In general, SSI can reduce the story shears up to more than 30% [7]. However, Table 13 shows that combination of torsional response with pounding and SSI can reverse the trend and increase the story shear response up to a value that is about 10% larger than that for the same building but on a rigid base. Therefore, there can be about 40% variation in the story shears for the cases studied in this paper.

6.5. The plastic hinge rotations

The resultant PHR's normalized to their fixed base counterparts are displayed in Fig. 14 for the whole stories of the buildings. The maximum resultant PHR within all eccentricity values without SSI for the 4-story building is 0.1109, 0.1395, and 0.1494 rad for d = 0, 0.5, and 1, respectively. The corresponding values for the 10-story building are 0.2121, 0.2136, and 0.2180 rad, respectively.

In Fig. 14, overall it is seen that the PHR values are more sensitive to the value of the clear distance ratio than the other responses. A similar conclusion has been drawn in Ref. [7] for ecc = 0%. Maximum PHR of

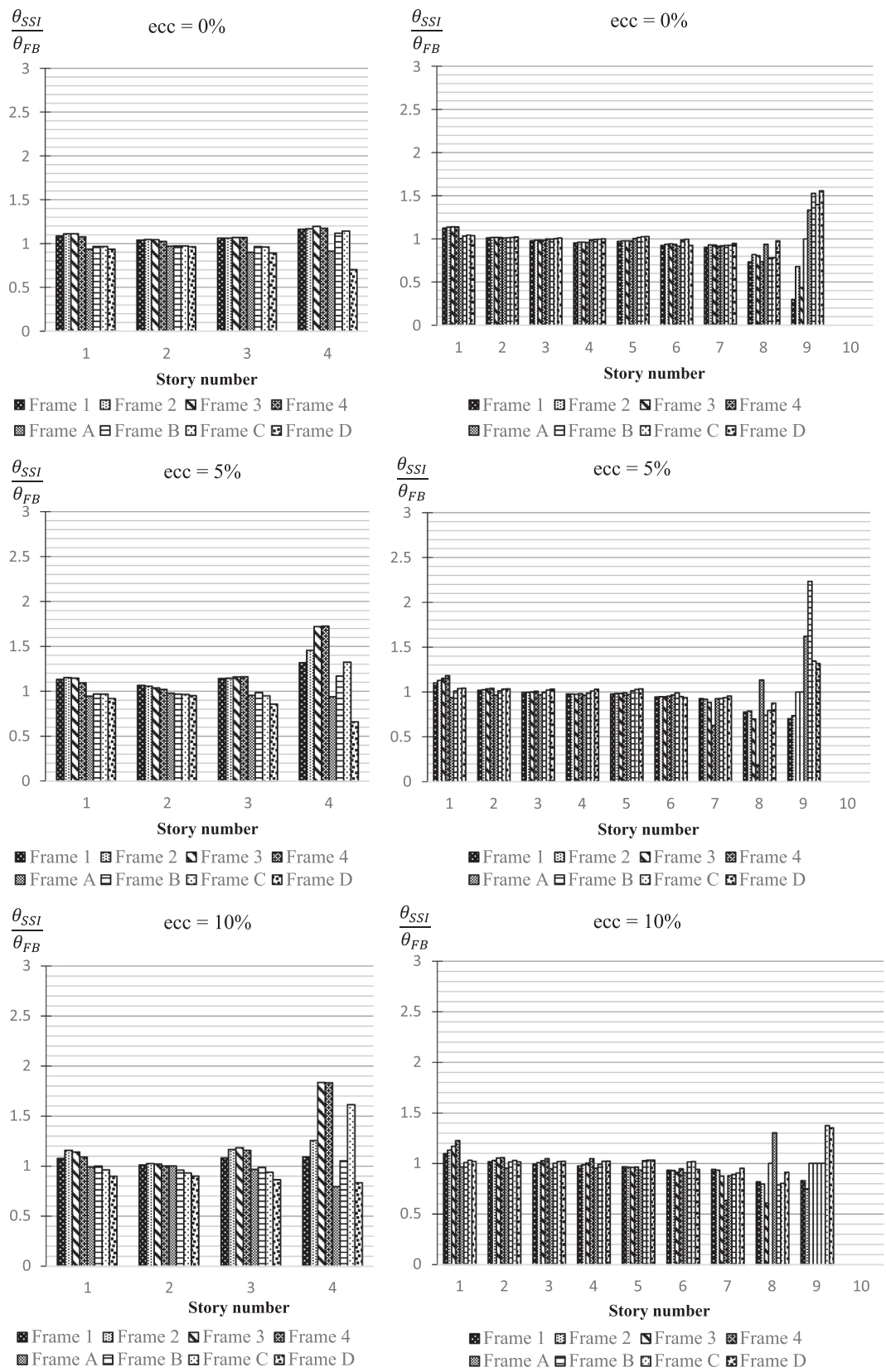

Fig. 16. The PHR ratios for each frame of the (4, 10) building pair with SSI normalized to those of similar frames without SSI for a clear distance ratio of 0.5.

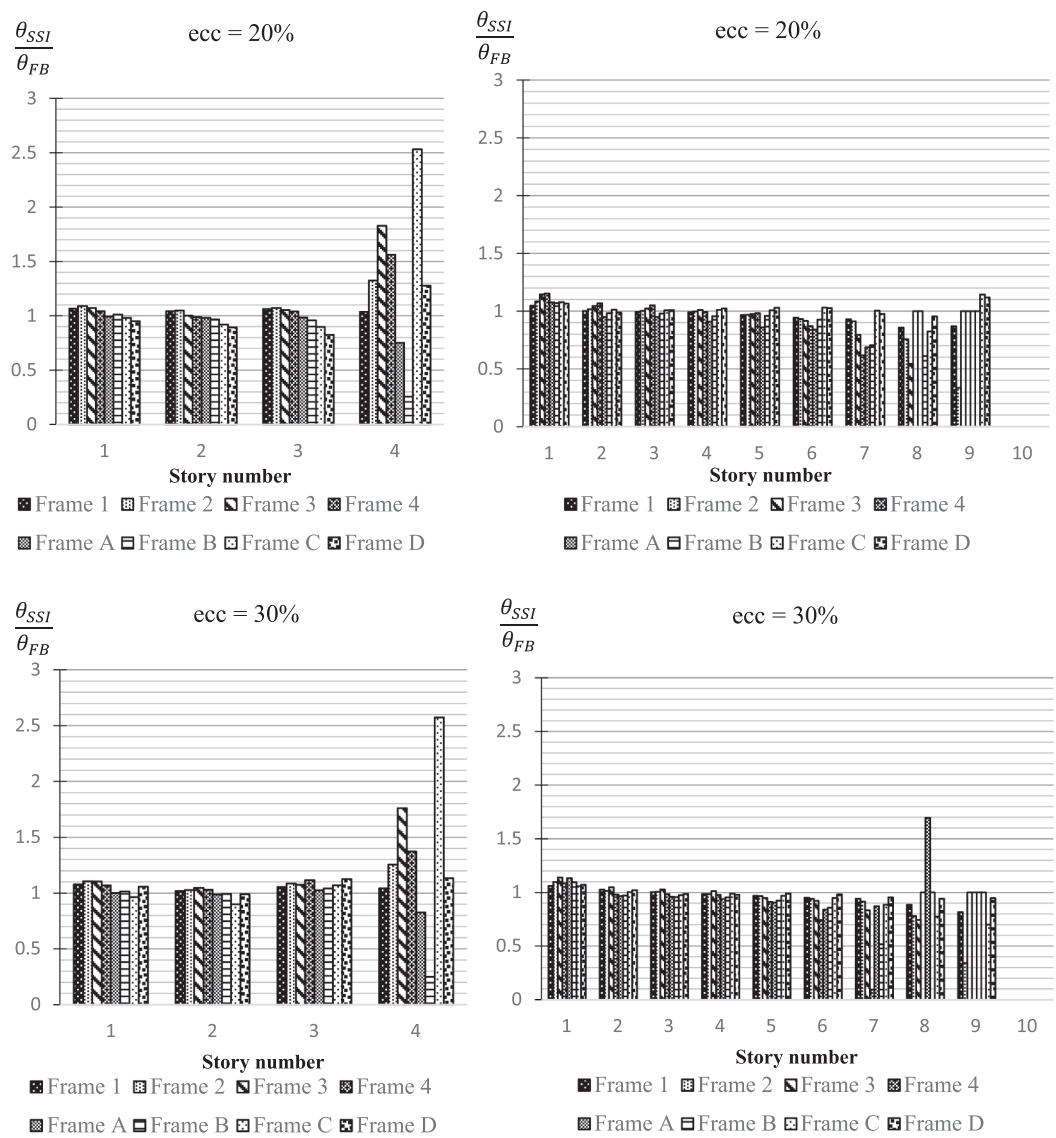

Fig. 16. (*continued*)

the buildings at different clear distances is observed at their top stories. It is because of the SSI effects and can be related to the foundation rotational displacement component. Foundation rotation increases displacements and accelerations at the upper stories. This value gradually reduces with increasing the clear distance for the case of shorter building where the pounding force and SSI are the major factors. Nevertheless, it is not the case for the taller building, because SSI is the main reason for increasing PHR at the top story of the taller building and the clear distance has minor influence on that. In addition, eccentricity has a reducing effect and the plastic response generally decreases with increasing the eccentricity ratio.

As mentioned in Table 2, the 10-story building rests on a 15 × 15 × 1 m mat foundation. Using the dynamic analysis of this study, the averaged maximum lateral displacement at the roof level of the 10-story building due to only rotation of its foundation and the residual roof displacement because of foundation rotation are calculated and presented in Table 14. The mentioned responses are small compared to the total response.

Results of the resultant PHR ratios are shown for each frame in Figs. 15–17.

According to the above figures, there are many cases in which SSI has increased the PHR considerably. This is more highlighted for individual frames. There are cases in which by increasing the torsional eccentricity, the PHR of the farther frames to the stiffness center multifolds with SSI. For instance, in the 4-story building, increase of the mentioned response in the perimeter frames is about 2.5 times at an eccentricity ratio of 30%. This fact exhibits the detrimental effect of combined torsion, SSI and pounding on plastic action of the frames. Moreover, as observed before, the rocking component of the foundation motion significantly increases the plastic response of the upper stories of the frames, especially for the taller building.

Table 15 summarizes the maximum ratios of PHR increments and decrements for the studied building pairs. A similar trend as of the (4, 10) building pair is observed for the other building pairs too and the maximum ratio of PHR occurs at the upper stories. It shows the fact that amplification of the nonlinear response is a serious problem for the torsional buildings on flexible bases. Therefore, more research in this regard is strongly recommended.

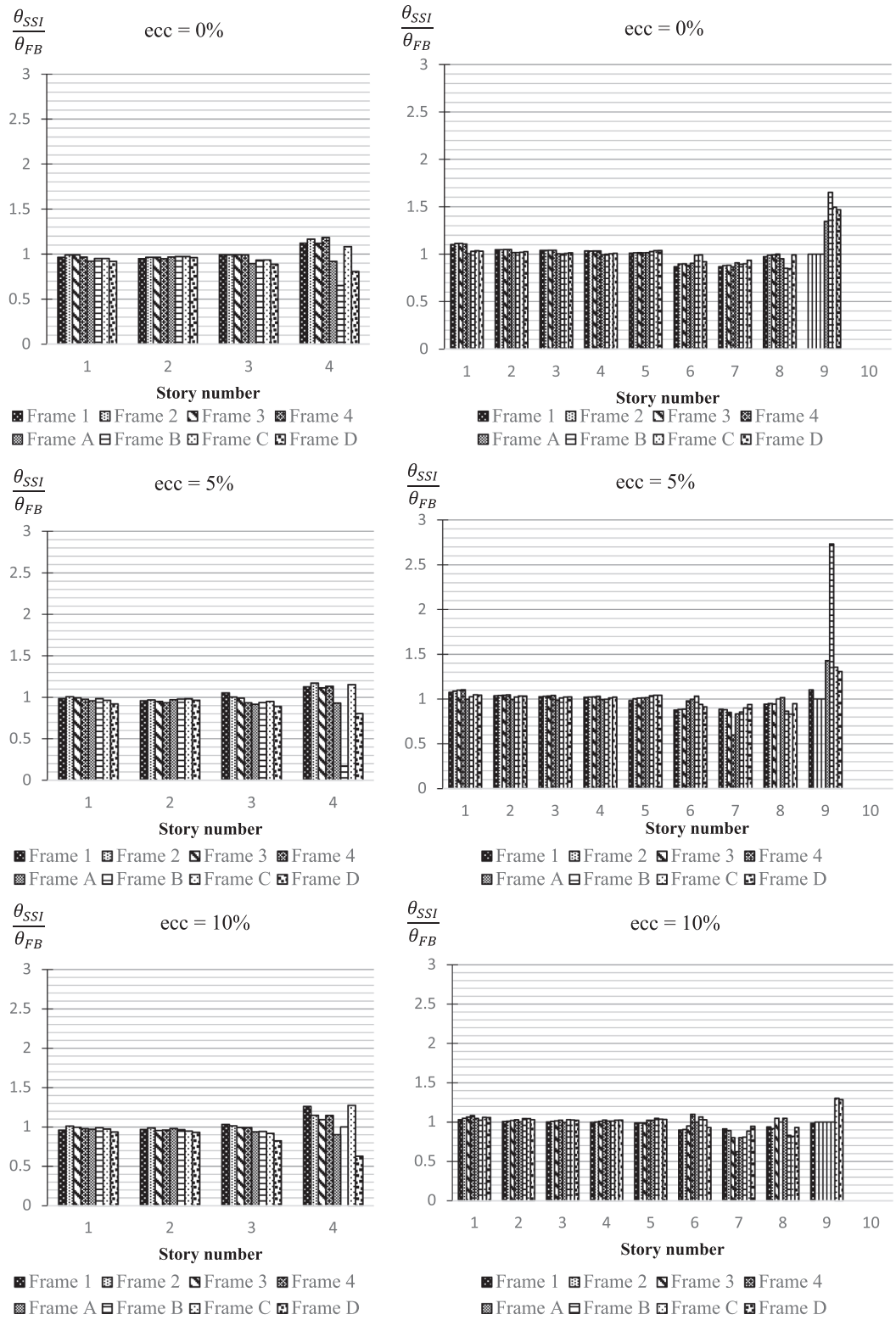

Fig. 17. The PHR ratios for each frame of the (4, 10) building pair with SSI normalized to those of similar frames without SSI for a clear distance ratio of 1.

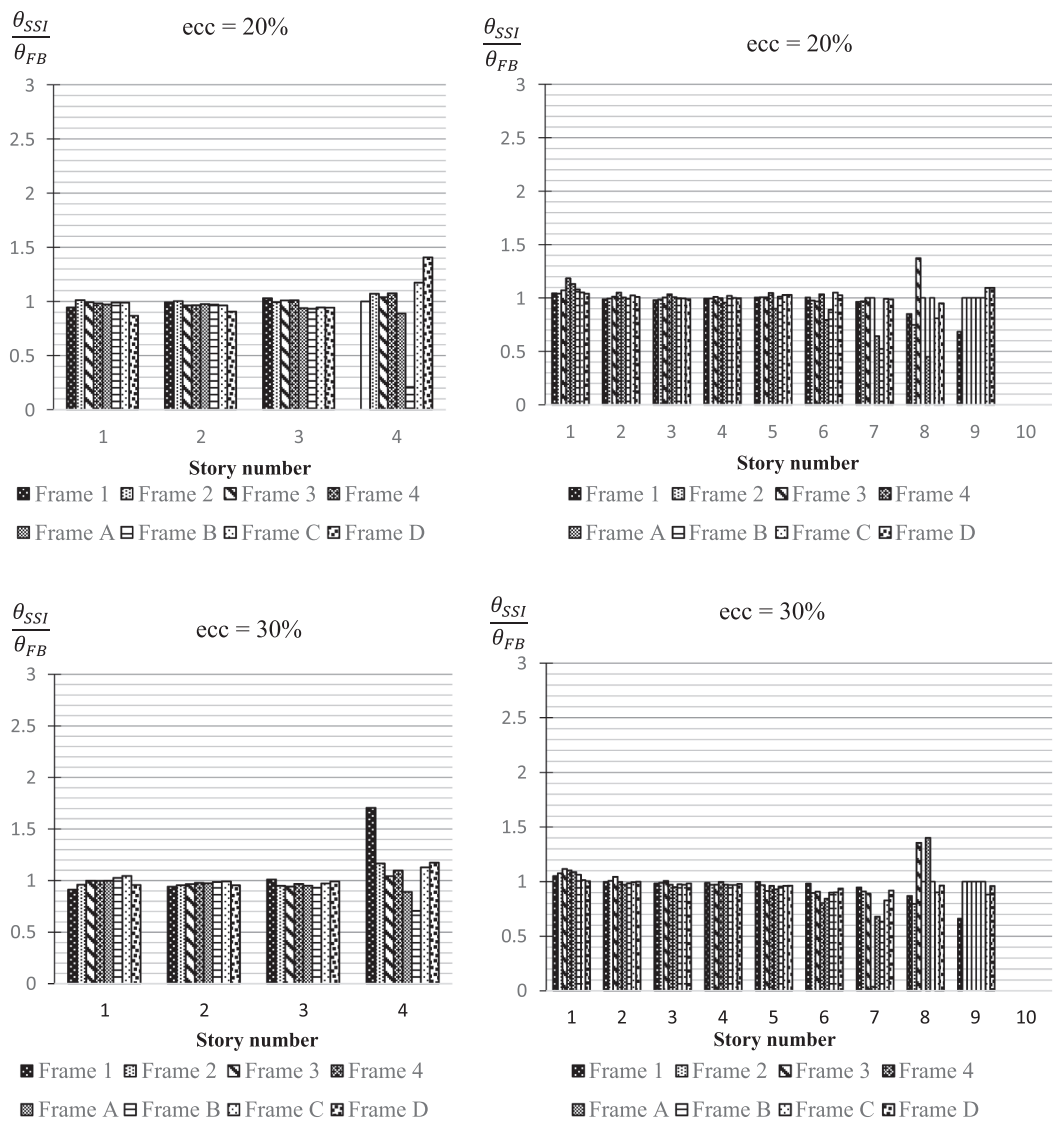

Fig. 17. (*continued*)

Table 15
Maximum percentages of decrease and increase of the story PHR's (RD and RI, respectively) for the building pairs normalized to their fixed-base associates.

Building pair	Shorter building			Taller building			Shorter building			Taller building		
	Ecc. (%)	Story	RD	Ecc. (%)	Story	RD	Ecc. (%)	Story	RI	Ecc. (%)	Story	RI
4, 4	30	4	13	–	–	–	0	4	12	–	–	–
4, 7	10	4	21	0	6	16	30	4	8	10	7	8
4, 10	0	3	5	30	9	14	5	4	32	0	9	46
7, 10	30	6	17	30	9	27	5	7	26	0	9	51
10, 10	30	9	37	–	–	–	0	9	70	–	–	–

7. Conclusions

The main goal of this study was investigating the concurrent effects of structure-soil-structure interaction, torsional eccentricity and pounding on the seismic responses of neighboring buildings. For this purpose, five pairs of steel moment-resisting frame buildings resting on a soft soil (i.e. site class D) were considered. Appropriate models were utilized to simulate the nonlinear behavior of the adjacent buildings including soil-structure interaction and structure-soil-structure interaction. Eleven ground motion pairs were selected and scaled for use in the nonlinear time history analysis. Building pairs were analyzed under the excitation of bi-directional ground motions and average of the maximum recorded responses were calculated. The results obtained from flexible-base models were normalized with respect to the corresponding fixed-base results in order to evaluate SSI and SSSI. Investigation of the aforementioned results led to the following conclusions:

1. There is no guarantee that following the code prescribed minimum separation distance would be enough to eliminate earthquake-induced pounding between adjacent buildings.
2. Structure-soil-structure interaction increases the number of occasions and amplitude of the pounding force in the lower half of the buildings.
3. Increasing the clear distance may reduce the seismic response of the shorter building. However, for the taller building, the responses are not influenced by the clear distance where SSI plays the main role for the amplified response of the upper stories.
4. Considering SSI notably increases the seismic responses at the upper stories as a result of the rotational component of the foundation.
5. Structure-soil-structure interaction has an important effect on the nonlinear response of the moment frames located at the perimeter of the torsionally coupled adjacent buildings. It can amplify the plastic action of such frames to more than two times in certain cases. It seems that a proper modeling of SSSI is necessary for such cases.
6. The torsional eccentricity does not have a uniform effect on the seismic response of the studied buildings.

References

[1] Mate NU, Bakre SV, Jaiswal OR. Seismic pounding of adjacent linear elastic buildings with various contact mechanisms for impact simulation. Asian J Civ Eng 2015;16:383–415.
[2] Jankowski R. Non-linear viscoelastic modelling of earthquake-induced structural pounding. Earthq Eng Struct Dyn 2005;34:595–611.
[3] Muthukumar S, DesRoches R. A Hertz contact model with non-linear damping for pounding simulation. Earthq Eng Struct Dyn 2006;35:811–28.
[4] Rahman AM, Carr AJ, Moss PJ. Structural pounding of adjacent multi-storey structures considering soil flexibility effects. 12th World Conf Earthq Eng Artic 2000.
[5] Mahmoud S, Abd-Elhamed A, Jankowski R. Earthquake-induced pounding between equal height multi-storey buildings considering soil-structure interaction. Bull Earthq Eng 2013;11:1021–48.
[6] Naserkhaki S, Aziz FNAA, Pourmohammad H. Earthquake induced pounding between adjacent buildings considering soil-structure interaction. Earthq Eng Eng Vib 2012;11:343–58.
[7] Madani B, Behnamfar F, Riahi HT. Dynamic response of structures subjected to pounding and structure–soil–structure interaction. Soil Dyn Earthq Eng 2015;78:46–60.
[8] Ghandil M, Aldaikh H. Damage-based seismic planar pounding analysis of adjacent symmetric buildings considering inelastic structure–soil–structure interaction. Earthq Eng Struct Dyn 2017;46:1141–59.
[9] Kontoni D-PN, Farghaly AA. Seismic response of adjacent unequal buildings subjected to double pounding considering soil-structure interaction. Computation 2018;6:10.
[10] Fatahi B, Van Nguyen Q, Xu R, Sun W. Three-dimensional response of neighboring buildings sitting on pile foundations to seismic pounding. Int J Geomech 2018;18:4018007.
[11] Pawar PD, Murnal PB. Effect of seismic pounding on adjacent blocks of unsymmetrical buildings considering soil-structure interaction. Int J Emerg Technol Adv Eng 2014;4:391–5.
[12] ASCE/SEI 7-10. Minimum design loads for buildings and other structures. Virginia: American Society of Civil Engineers (ASCE); 2010.
[13] ANSI/AISC 360-10. Specification for structural steel buildings. Am Inst Steel Constr; 2010.
[14] ACI Committee 318. Building code requirements for structural concrete (ACI 318-14) and commentary (ACI 318R-14); 2014. doi: 10.1016/0262-5075(85)90032-6.
[15] Mazzoni S, McKenna F, Scott MH, Fenves GL. OpenSees command language manual. Berkeley, CA: University of California at Berkeley; 2006.
[16] Maison BF, Kasai K. Dynamics of pounding when two buildings collide. Earthq Eng Struct Dyn 1992;21:771–86.
[17] Anagnostopoulos SA. Pounding of buildings in series during earthquakes. Earthq Eng Struct Dyn 1988;16:443–56.
[18] Anagnostopoulos SA. Equivalent viscous damping for modeling inelastic impacts in earthquake pounding problems. Earthq Eng Struct Dyn 2004;33:897–902.
[19] Jankowski R, Mahmoud S. Earthquake-induced structural pounding. Springer; 2015.
[20] Harden CW, Hutchinson T, Martin GR, Kutter BL. Numerical modeling of the nonlinear cyclic response of shallow foundations. Pacific Earthquake Engineering Research Center 2005.
[21] Boulanger RW, Curras CJ, Kutter BL, Wilson DW, Abghari A. Seismic soil-pile-structure interaction experiments and analyses. J Geotech Geoenviron Eng 1999;125:750–9.
[22] Das BM. Principles of foundation engineering. Cengage learning 2015.
[23] ASCE. Seismic evaluation and retrofit of existing buildings (ASCE 41-13); 2014. doi: 10.1061/9780784412855.
[24] Mulliken JS, Karabalis DL. Discrete model for dynamic through-the-soil coupling of 3-D foundations and structures. Earthq Eng Struct Dyn 1998;27:687–710.
[25] Farahani D. Study on pounding in torsional adjacent buildings considering soil-structure interaction. Isfahan University of Technology; 2017.